LATERAL STRESS EFFECTS ON LIQUEFACTION RESISTANCE CORRELATIONS

Kenji Harada[1], Rolando P. Orense[2], Kenji Ishihara[3] and Jun Mukai[4]

SUMMARY

When the sand compaction pile (SCP) method is implemented to improve loose deposits of sandy soils, its effect is evaluated generally in terms of increase in density, which is beneficial for reducing the liquefaction potential of the deposits during earthquakes. An additional advantage can be expected to occur due to concurrent increase in lateral stress. When the resistance to liquefaction is evaluated on the basis of SPT *N*-value or CPT q_c-value, the increased resistance to penetration due to the sand compaction has been interpreted conventionally as being associated mainly with the increase in density. Therefore, in order to properly evaluate the effectiveness of ground improvement in compacted soils, it is necessary to quantify the effect of lateral stresses on the penetration resistance and liquefaction strength. In this paper, based on the results of SPT and CPT performed in a chamber box in the laboratory, the relationships between penetration resistance, liquefaction resistance and relative density were re-examined and the influence of lateral stress, expressed in terms of K_C, was investigated. Although the results indicated that generally the resistance to liquefaction increases with increasing K_C–value, little difference was noted when the density of the deposit was high. Based on the results, recommended charts incorporating the effect of K_C were proposed.

INTRODUCTION

Conventionally, the cyclic resistance to liquefaction of in-situ deposits is evaluated from the penetration resistance obtained using standard penetration tests (SPT) or cone penetration tests (CPT). In North America, for example, charts have been proposed by correlating the SPT *N*-value or CPT q_c-value and the estimates of cyclic stress ratio of a number of sites which had or had not manifested evidence of liquefaction during major earthquakes in the past (e.g., Youd *et al.,* 2001). In Japan, on the other hand, the results of cyclic shear tests on high-quality undisturbed samples from in-situ sand deposits are correlated with the penetration resistance obtained at nearby sites to establish the chart (e.g., JRA, 1996). Charts obtained from North American and Japanese practice tacitly assume that the lateral stress σ'_h in the deposit are approximately equal to 0.45-0.50 times the vertical effective stress, σ'_v; in other words, the lateral stress ratio, $K_C = \sigma'_h/\sigma'_v$, is taken as 0.45-0.50.

When liquefaction potential is to be evaluated for natural or reclaimed sand deposits, the above assumption may be reasonable. However, when these deposits are improved by means of a sand compaction pile (SCP) or any similar methods, it has been common practice to evaluate the effect of improvement in terms of the resistance in penetration tests, which is considered mainly to reflect an increase in density of sand deposits. However, opinions have been expressed that the pile installation and the resulting expansion of pile diameter during SCP implementation contribute to increased lateral stress in the deposits as well, which is known to be beneficial for further increasing resistance to liquefaction. Therefore, the effect of increased lateral stress needs to be properly accounted for in evaluating the liquefaction resistance of sand deposits.

In this paper, investigation is made on the effect of increased lateral stress on the cyclic resistance of sandy deposits. Since it is difficult to explicitly investigate the effects of the K_C–conditions on the relation between penetration resistance and relative density for natural grounds, results of various chamber tests performed in the laboratory were used instead. Thus, an attempt is made in the present study to seek such relations by compiling the results of chamber tests that have been reported so far, where the effect of K_C–conditions was examined explicitly. By analyzing the chamber test results taking into account the effects of K_C–condition and by establishing relations between relative density, penetration resistance and liquefaction resistance, design charts were formulated. These charts can serve as a guideline on how to incorporate the lateral stress condition in evaluating the liquefaction resistance of deposits improved by compaction methods.

EFFECTIVENESS OF SAND COMPACTION PILE METHOD

The sand compaction pile method is one of the popular methods for improving ground to resist liquefaction. As

[1] *General Manager, Fudo Tetra Corporation, Tokyo, Japan*

[2] *Senior Lecturer, Department of Civil and Environmental Engineering, University of Auckland, New Zealand (member)*

[3] *Professor, Department of Civil Engineering, Chuo University, Ube, Japan*

[4] *Senior Engineer, Fudo Tetra Corporation, Tokyo, Japan*

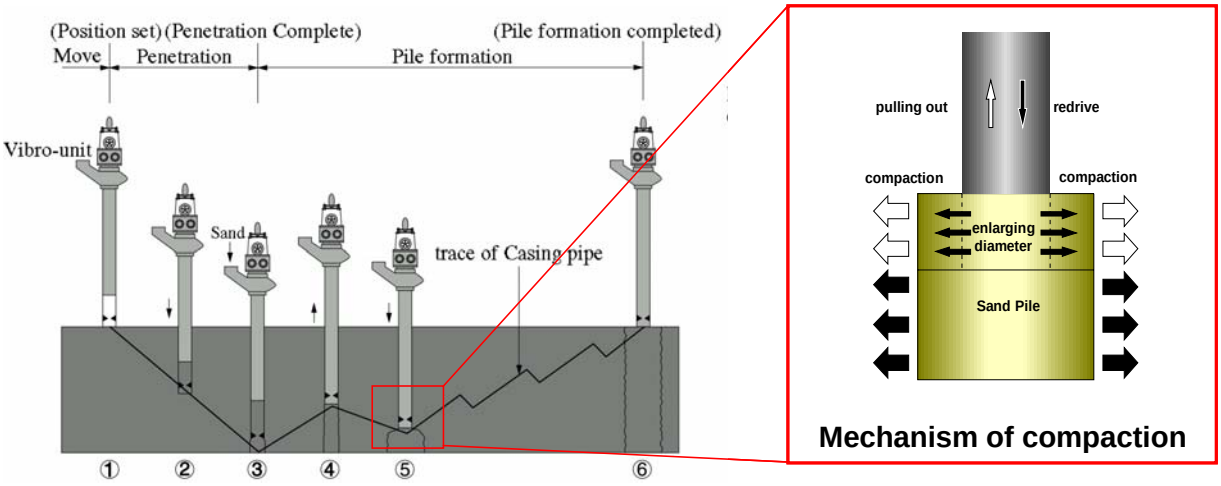

Figure 1: Procedure of installing sand compaction piles.

illustrated in Fig. 1, this method involves the installation of well-compacted sand piles of large diameters into the loose liquefiable sandy deposit through the process of repeated driving down and the extracting motion of a vibrating steel pipe. As the sand pile is compacted and enlarged, the adjacent ground is pushed laterally and compacted. The effectiveness of ground improvement is commonly assessed by evaluating the increase in the penetration resistance at the centre-point between the sand piles, which is considered to reflect mainly the increase in density of the ground.

To illustrate such increase in density, typical SPT *N*-values obtained from sites improved by both vibratory SCP and non-vibratory (Nv) SCP procedures are shown in Fig. 2(a) while examples of CPT q_c values from vibratory and non-vibratory (Nv) SCP–improved ground are illustrated in Fig. 2(b). It is observed that penetration resistances obtained between the installed sand piles are increased as the piles laterally pushed and displaced the adjacent sandy ground.

Moreover, results of cases where various instruments (e.g., pressuremeters and dilatometers) were used to measure the lateral stresses before and after implementation of both vibratory and non-vibratory SCP methods are presented in Fig. 3. In the figure, the relation between the lateral stress ratio, K_C, and improvement ratio, a_s, is plotted 2 years and 1 month after the SCP operation. Note that the data points corresponding to a_s=0 refer to the condition prior to the implementation of SCP method. The trend shows that substantial increases in K_C–values are observed after SCP implementation, with larger increases in K_C–values occurring at higher a_s.

BASIC CONSIDERATIONS

In order to establish design charts relating the penetration resistance and the liquefaction resistance, but which would incorporate explicitly the influence of K_C–conditions, the following methodology was adopted in this study:

(1) Firstly, the relationship between the liquefaction resistance *R* and the penetration resistance, expressed in terms of penetration resistance normalised with respect to an effective overburden pressure of σ'_v = 1 kgf/cm^2 or 98 kPa (i.e., SPT N_1-value or q_{c1}-value), have been proposed and used both in Japan and in North America. As mentioned earlier, it can be assumed with good reasons that these relations between *R* and N_1 or q_{c1} are applicable for soil deposits consolidated under K_C =0.5 condition. These will therefore serve as the reference relationship in investigating the effects of various K_C–conditions.

(2) It was necessary to express both *R* and N_1 or q_{c1} value as

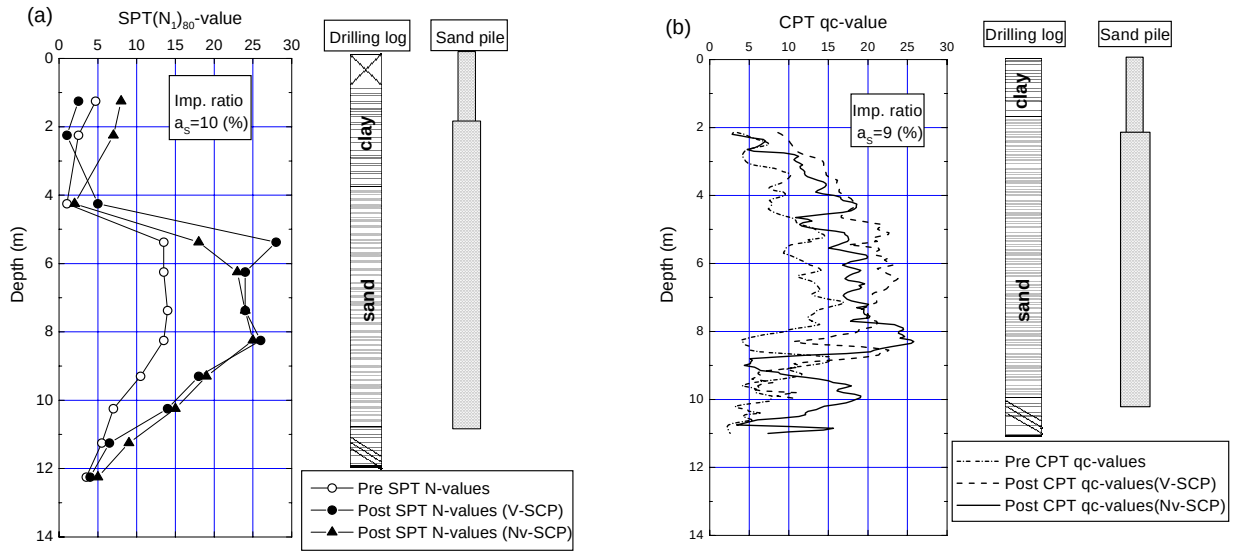

Figure 2: Examples of increased penetration resistances in grounds improved by the SCP method in terms of: (a) SPT N–values; and (b) CPT q_c–values.

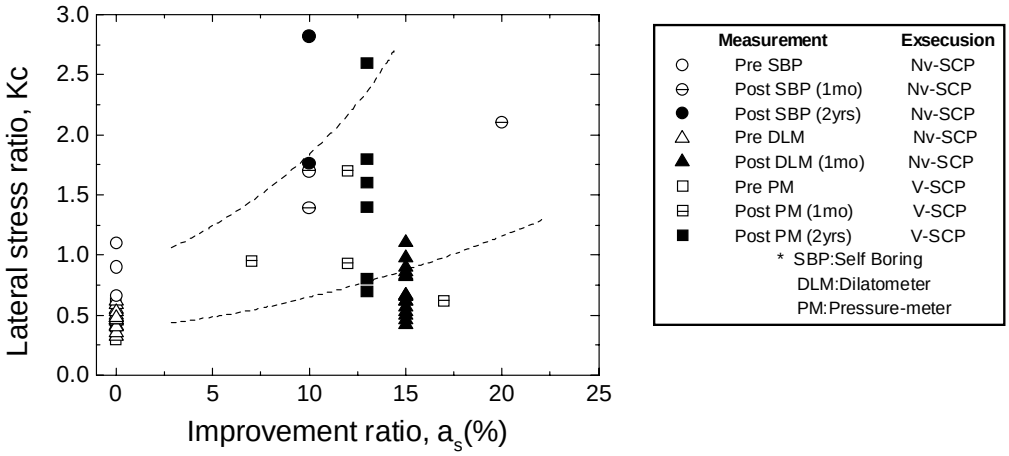

Figure 3: Example of results showing increase in K_C–values due to SCP implementation.

a function of the relative density, D_r, considering K_C=0.5 condition. For this purpose, results of chamber tests, where D_r was utilized to express the state of looseness or denseness of the sand employed, and correlations which are available in the literature, were used to develop the required relationships.

(3) Next, the results of calibration chamber tests were analyzed in which SPT N–value or cone penetration resistance q_c is measured under controlled K_C–conditions for sand deposits prepared at different relative densities. Thus, the penetration resistance (q_{c1} or N_1 values) is expressed in terms of the relative density, D_r, and K_C–value. Moreover, a relationship showing the K_C–effects on liquefaction resistance (Ishihara and Takatsu, 1979) was used to establish the effects of K_C–conditions on the liquefaction resistance R under different relative densities.

(4) Finally, with the above two kinds of relations ready for use, it would then be possible to eliminate the relative density between them and to obtain direct relations between the liquefaction resistance R and penetration resistance q_{c1} or SPT N_1–value for different K_C–values.

The details of the above procedure are summarized in the flowchart illustrated in Fig. 4. In pursuing the above approach, it is to be noticed that the basic data sets used in the study were obtained from the tests on samples or deposits artificially prepared in the laboratory. In comparison, there is practically no data available showing the effects of K_C–value on in-situ deposits. Therefore, the following assumptions are made to support the methodology presented above:

Firstly, the outcome of the torsional tests in the laboratory on reconstituted samples of clean sands by Ishihara and Takatsu (1979) and Harada *et al.* (2000) disclosed the relationship given below.

$$\left[\frac{(R)_{K_C}}{(R)_{1.0}}\right]_{lab.} = \frac{1+2K_C}{3} \qquad (1)$$

where $(R)_{1.0}$ and $(R)_{KC}$ denote, respectively, the liquefaction resistance under K_C =1.0 (isotropic) and other K_C–conditions. Without knowing the similarly defined relationship for field conditions, it is necessary to make an assumption regarding the effects of K_C–conditions as follows.

$$\left[\frac{(R)_{K_C}}{(R)_{1.0}}\right]_{field} \cong \left[\frac{(R)_{K_C}}{(R)_{1.0}}\right]_{lab.} \qquad (2)$$

This relationship may not generally hold valid, because there are a variety of factors such as ageing and cementation in the field deposits. However, if a K_C–condition is produced as a result of mechanical actions such as the sand compaction pile in the field, the relationship given by Eq. (2) may be considered reasonable in correlating in-situ and laboratory-produced conditions. Nevertheless, tests are necessary to

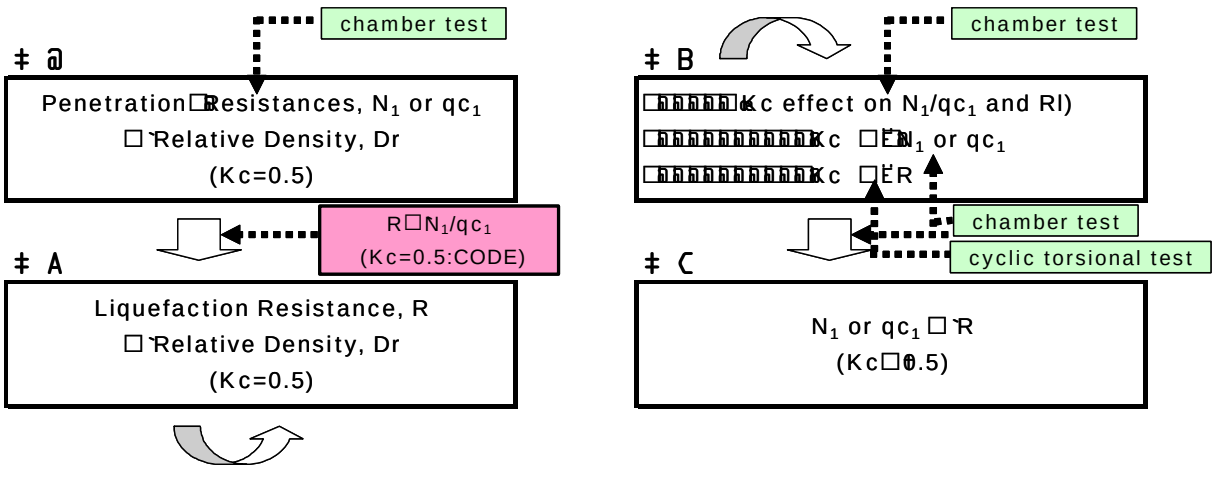

Figure 4: Flowchart used in evaluation.

validate the assumption made in Eq. (2).

Secondly, the soil deposit inside the calibration chamber where penetration testing was conducted was also prepared by pluviating dry sands or by sedimenting sands under water. Since there has been no attempt ever made to quantify the effect of K_C–condition for in-situ deposits of sands, it would be necessary to have the following assumption as formulated below.

$$\left[\frac{(q_{c1})_{K_C}}{(q_{c1})_{1.0}}\right]_{field} \cong \left[\frac{(q_{c1})_{K_C}}{(q_{c1})_{1.0}}\right]_{lab.} \quad (3a)$$

$$\left[\frac{(N_1)_{K_C}}{(N_1)_{1.0}}\right]_{field} \cong \left[\frac{(N_1)_{K_C}}{(N_1)_{1.0}}\right]_{lab.} \quad (3b)$$

As mentioned above, this correlation between field and laboratory conditions may be taken as reasonable, when the K_C–value is changed by a mechanical action such as implementation of the sand compaction technique.

REFERENCE RELATIONS FOR NORMALLY CONSOLIDATED CONDITION

As mentioned earlier, the resistance to liquefaction of sand deposits during earthquakes has been investigated extensively and expressed in the form of charts correlating the liquefaction resistance R and penetration resistance, either by standard penetration or cone penetration tests.

In Japan, efforts have been expended towards obtaining high-quality undisturbed samples from in-situ sand deposits and testing them in the laboratory by means of cyclic triaxial test apparatus. The results of the tests were combined with the SPT N–values at respective nearby sites to establish the chart. In the formula incorporated in the Japanese code, the liquefaction resistance, R, corresponding to a shaking which is expected to occur in an earthquake involving the subduction type of plate movement (one generally adopted in practice) is expressed as a function of SPT N–value as follows (JRA, 1996).

$$R = \begin{cases} 0.0882\sqrt{(N_1)_{80}/1.7} & (N_1)_{80} < 14 \\ 0.0882\sqrt{(N_1)_{80}/1.7} + 1.6\times10^{-6}((N_1)_{80}-14)^{4.5} & (N_1)_{80} \geq 14 \end{cases} \quad (4)$$

In the above equation, N_1 value is the corrected SPT N–value for an effective overburden pressure, σ'_v = 1 kgf/cm^2 (or 98 kPa) by way of the formula $N_1 = (1.7N)/(0.7+\sigma'_v)$. Moreover, the subscript 80 refers to the effective energy in hammer dropping, which is considered as approximately equal to 80% of the theoretical energy based on Japanese practice. This correlation is an outgrowth of an enormous amount of work, including undisturbed sampling by freezing techniques and laboratory testing. In the Japanese code, the cyclic stress ratio causing 5% double-amplitude axial strain in 20 cycles of uniform loading is obtained in the triaxial test under isotropic condition (K_C = 1.0). Then, it is corrected for the K_C = 0.5 condition by multiplying (1+2K_C)/3 = 2/3 and also for the peak value of shear stress in irregular time histories of seismic excitation by multiplying 1.5. Thus, the value of R obtained by Eq. (4) is considered to represent the cyclic strength in terms of the peak shear stress divided by the effective overburden pressure in the K_C = 0.5 condition.

In North American practice, on the other hand, this type of relation has been exploited mainly based on field observations of a number of sites, which had or had not manifested evidence of liquefaction during major earthquakes in the past. In terms of the cyclic resistance ratio (*CRR*), which is commonly used there, the liquefaction resistance can also be expressed as (Youd *et al.*, 2001):

$$R = \frac{CRR}{0.65} = \frac{1}{0.65}\left[\frac{1}{34-(N_1)_{60}} + \frac{(N_1)_{60}}{135} + \frac{50}{[10-(N_1)_{60}+45]^2} - \frac{1}{200}\right] \quad (5)$$

Note that in the above equation, which is valid for $(N_1)_{60}$<30, an approximate relation $(N_1)_{60} = 1.3(N_1)_{80}$ can be incorporated to correct for the difference in energy transfer between the Japanese and American SPT practice. Moreover, the correcting factor 0.65 indicated in Eq. (5) was used to take into account the fact that the liquefaction resistance in Japanese code is expressed in terms of the maximum value of acceleration, while the average value of acceleration during seismic shaking is used in American practice.

In similar vein, the formula for the liquefaction resistance, R, as a function of the q_{c1}–value as proposed by Suzuki and Tokimatsu (2003) is expressed as follows,

$$R = \frac{1}{0.65}\frac{\tau_\ell}{\sigma_o'} = \frac{1}{0.65}\left\{0.45\times0.57\times\left[\frac{16\sqrt{N_c}}{100} + \left(\frac{16\sqrt{N_c}}{83.7}\right)^{14}\right]\right\}$$

$$\text{where} \quad N_c = \begin{cases} 0.341{I_c}^{1.94}(q_{c1}-0.2)^{1.34-0.0927I_c} & q_{c1} > 0.2\,\text{MPa} \\ 0 & q_{c1} \leq 0.2\,\text{MPa} \end{cases} \quad (6)$$

In the above equation, I_c is the CPT soil type behaviour index and q_{c1} is the cone resistance corrected for an effective overburden pressure, σ'_v =1 kgf/cm^2 (or 98 kPa) with the equation $q_{c1} = q_c/(\sigma'_v)^{0.5}$. On the other hand, the relationship between R and q_{c1} based on North American practice is given by Robertson and Wride (1998). When expressed in SI units, the curve can be approximated by the following equations:

$$R = \frac{CRR}{0.65} = \begin{cases} 0.0134(q_{c1}) + 0.077 & \text{for } q_{c1} < 4.8\,\text{MPa} \\ 1.63\times10^{-4}(q_{c1})^3 + 0.123 & \text{for } 4.8 \leq q_{c1} < 15.3\,\text{MPa} \end{cases} \quad (7)$$

In the above equations, it is tacitly assumed that the lateral stress ratio in the sand deposit would be approximately equal to K_C = 0.50. Thus, Eqns (4–7) will serve as the reference relations in investigating the effects of various K_C–conditions.

PENETRATION RESISTANCE AND RELATIVE DENSITY RELATION

As a first step, a discussion on the relationship between penetration resistance and relative density is presented for the case of K_C = 0.5. Firstly, considering various types of soils, Cubrinovski and Ishihara (1999) proposed a relationship between the mean grain size, D_{50}, and the void ratio range, e_{max}–e_{min}, as shown below, where e_{max} and e_{min} are the maximum and minimum void ratios, respectively.

$$e_{max} - e_{min} = 0.23 + \frac{0.06}{D_{50}} \quad (8)$$

In the analysis presented herein, only the results for clean sands are considered, and the sands are classified roughly as being either fine sand or coarse sand. For fine sand, the mean grain diameter will be taken as D_{50} = 0.2~0.3 mm with e_{max}–e_{min} = 0.4~0.5 (average = 0.45) while values of D_{50} = 0.3~0.5 mm and e_{max}–e_{min} = 0.35~0.4 (average = 0.375) will be assumed for coarse sand.

Corrected *N*–value and Relative Density

Several researchers have investigated the relationship between SPT N–value and relative density, D_r. Among these, the data compiled by Fujita (1968) are considered the most comprehensive and these are shown in Fig. 5(a). Additional data points are plotted from the results of chamber tests conducted by Yoshida *et al.* (1988), Yasuda *et al.* (1996) and

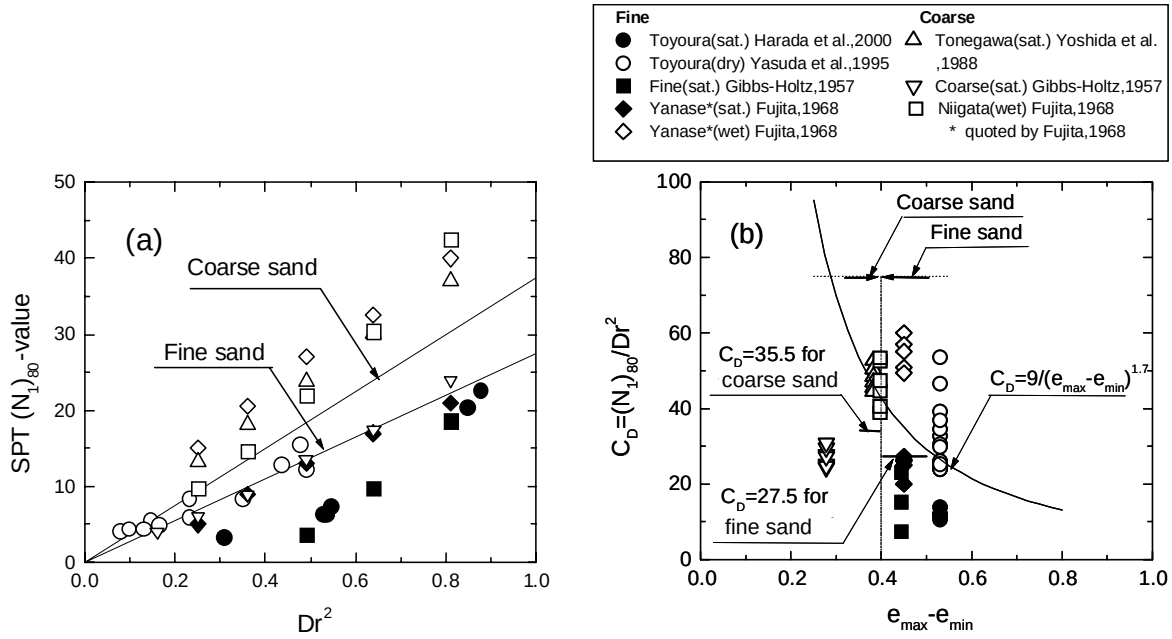

Figure 5: (a) Relationship between SPT $(N_1)_{80}$-value and relative density, D_r; and (b) Relationship between $(N_1)_{80}/D_r^2$ and void ratio range.

other investigators. Since all the data were obtained from chamber tests, the energy transfer ratio in the hammer dropping is considered approximately equal and assumed as 80%. Note that because the test implementation is similar in both chamber and field conditions, it is reasonable to assume that a similar energy efficiency can be used in both conditions. The blow count number thus obtained is indicated as $(N_1)_{80}$. Both fine and coarse sands are included in the figure, as well as saturated and dry/wet soils. It may be observed that a linear relationship can be roughly established between $(N_1)_{80}$ and the square of D_r expressed as a ratio, not a percentage, with fine and dry sands showing higher gradients than coarse sands and dry/wet samples. It is to be recalled that the linearity between N_1 and D_r^2 is consistent with the relation of $N_1 = 40D_r^2$, proposed by Meyerhof (1957).

Next, the slope of a straight line connecting the zero point and each of the data point in Fig. 5(a) is read off and plotted versus the value of e_{max}–e_{min} for each of the sands used in the chamber tests. This slope, as indicated by C_D, is shown in the ordinate of Fig. 5(b). The solid curve in the figure is the average of the data points compiled by Cubrinovski and Ishihara (1999). It can be observed that although the data points for saturated and dry/wet samples show different trends, all the data points may be represented roughly by the following expression as proposed by Cubrinovski and Ishihara (1999):

$$(N_1)_{80} = C_D \cdot D_r^{\,2} = \frac{9}{(e_{max} - e_{min})^{1.7}} \cdot D_r^{\,2} = \frac{9}{\left(0.23 + \frac{0.06}{D_{50}}\right)^{1.7}} \cdot D_r^{\,2} \qquad (9)$$

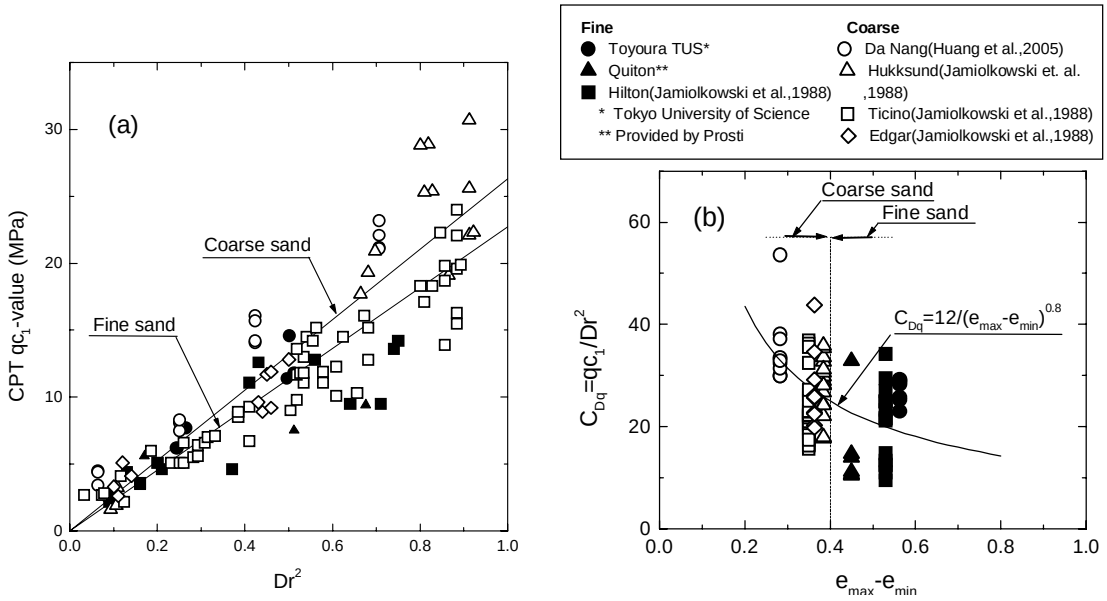

Figure 6: (a) Relationship between q_{c1}-value and relative density, D_r; and (b) Relationship between q_{c1}/D_r^2 and void ratio range.

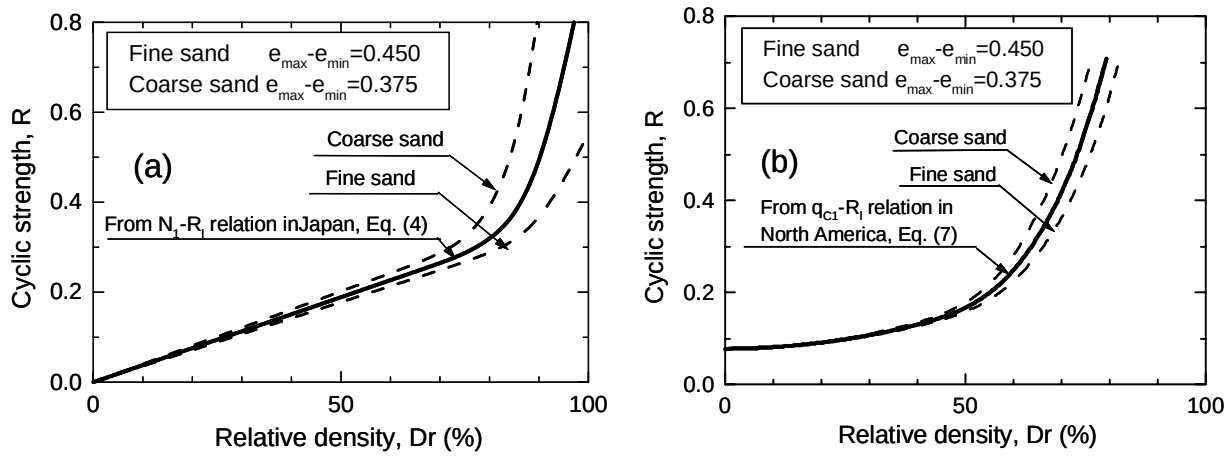

Figure 7: Relationship between liquefaction resistance and D_r: (a) from N_1 value; and (b) from q_{c1} value.

where the relationship of Eq. (8) is used to account for the gradation effects of each sand. It can be seen in Fig. 5(b) that there is considerable scatter in the data points but, for practical purposes, the values of C_D may be taken roughly as 27.5 and 35.5 for fine and coarse sands, respectively.

Corrected q_c–value and Relative Density

Similar to that performed for SPT N–values, the data of cone resistance corrected for an effective overburden pressure, σ'_v =1 kgf/cm^2 (or 98 kPa) are shown in Fig. 6(a) versus D_r^2. These were obtained from various test results (Jamiolkowski *et al.*, 1988; Huang and Hsu, 2005). All the data points indicated in the figure are for dry samples. Note that unlike the case shown in Fig. 5(a), there is no significant difference between the trends for fine sands and coarse sands. The relation between the slope of this plot (q_{c1}/D_r^2) and the void ratio range, similarly established, is shown in Fig. 6(b). For each of the data points, it may be seen that the effect of grain diameter is insignificant. Thus, similar to the empirical equation of Eq. (9), the relation between q_{c1} and D_r may be expressed as follows:

$$q_{c1} = C_{Dq} \cdot D_r^{\,2} = \frac{12}{(e_{\max} - e_{\min})^{0.8}} \cdot D_r^{\,2} = \frac{12}{\left(0.23 + \dfrac{0.06}{D_{50}}\right)^{0.8}} \cdot D_r^{\,2} \qquad (10)$$

It is to be noted that there are relations of the form D_r versus log q_{c1} proposed by Jamiolkowski *et al.* (1988), but the form of Eq. (10) will be used instead in this study.

LIQUEFACTION RESISTANCE AND RELATIVE DENSITY RELATION

From SPT Tests

The relationship between $(N_1)_{80}$ and D_r, given by Eq. (9), is substituted into Eqs. (4) and (5) to obtain the relationship between R and D_r. The plots thus obtained from Eq. (4) for the Japanese code are displayed in Fig. 7(a), corresponding to fine sand and coarse sand. Similar plots can be obtained from Eq. (5), but they are not shown here. It can be observed in Fig. 7(a) that the liquefaction resistance shows a sudden increase when the relative density is greater than about D_r = 90% for fine sand and when D_r is larger than 80% for coarse sand.

From CPT Tests

Similarly, the relationship between the q_{c1} value and D_r given by Eq. (10) is substituted into Eqs. (6) and (7) to obtain the relationship between R and D_r. The plots thus obtained from Eq. (7) are shown in Fig. 7(b) for fine and coarse sands. The relationship from Eq. (6) can be similarly obtained, but is not shown here. It is seen in Fig. 7(b) that the liquefaction resistance shows a sudden increase when the density exceeds D_r = 60% for both fine and coarse sands.

As there is not much difference between the curves for fine and coarse sands in both figures, the average curves shown by the solid lines in Fig. 7 will be adopted hereafter.

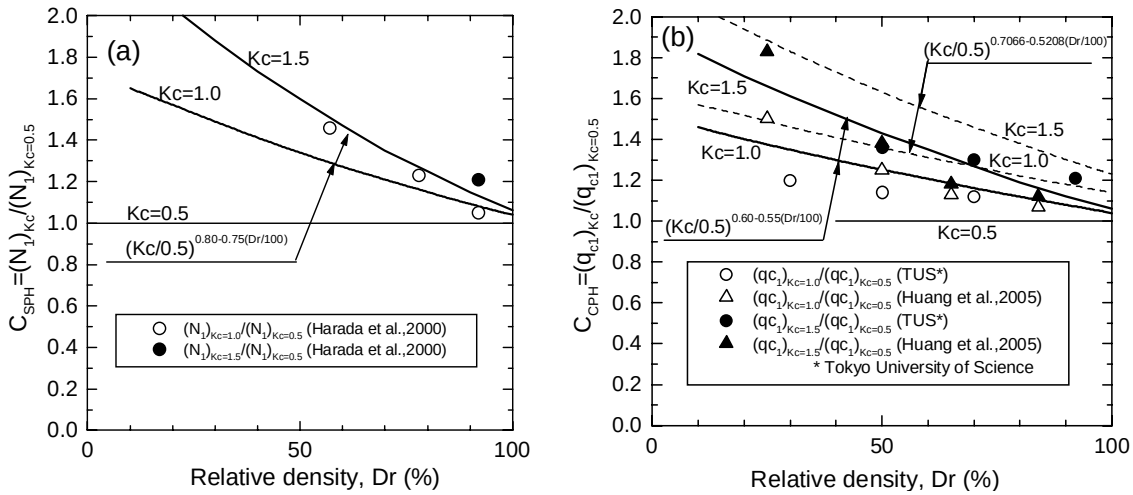

Figure 8: Relation between relative density and increase in penetration resistance (a) SPT data; and (b) CPT data.

EFFECT OF K_C ON PENETRATION RESISTANCE AND LIQUEFACTION RESISTANCE

Effect of K_C on Penetration Resistance

K_C–effect on SPT

There has been no data ever reported in the literature on the effects of K_C–conditions on SPT N–values, except for the recent data obtained at the Tokyo Denki University. This data is shown in Fig. 8(a) in terms of C_{SPH} defined as the increase in standard penetration resistance associated with increase in K_C–value, i.e., $C_{SPH} = (N_1)_{KC}/(N_1)_{KC=0.5}$ which is plotted versus the relative density (expressed in %). One set of data pertains to the values of C_{SPH} when K_C was increased from 0.5 to 1.0 and another set was for the case of K_C = 0.5 to 1.5. From the data, the following relationship, given by Eq. (11), is proposed. This relationship is shown by the lines in Fig. 8(a). Note that these lines were drawn to best-fit the data points for denser state of saturated Toyoura sand in Fig. 5(a).

$$C_{SPH} = \left(\frac{K_C}{K_{C,NC}} \right)^{0.80-0.75(D_r/100)} \tag{11}$$

K_C–effect on CPT

Various relationships have been proposed based on the chamber test results indicating the effect of K_C on the q_c–values of CPT. These are as follows:

Salgado (1997):

$$C_{CPH} = \sqrt{\frac{K_C}{K_{C,NC}}} \tag{12}$$

Jamiolkowski et al. (1988); Huang & Hsu (2005):

$$C_{CPH} = \sqrt{\frac{1+2K_C}{1+2K_{C,NC}}} \tag{13}$$

Boulanger (2003):

$$C_{CPH} = \left(\frac{K_C}{K_{C,NC}} \right)^{0.7066-0.5208(D_r/100)} \tag{14}$$

where C_{CPH} indicates the increase in cone penetration resistance associated with an increase in K_C–value, i.e., $C_{CPH} = (q_{c1})_{KC}/(q_{c1})_{KC=0.5}$. The subscript NC represents normally consolidated condition (i.e., K_C = 0.5). Eqs. (12) and (13) indicate constant values for any changes in the value of K_C irrespective of the relative density. However, Eq. (14) indicates that the parameter C_{CPH} tends to decrease with increasing relative density (expressed in %), which appear more reasonable in the light of the results of recent tests.

The values of C_{CPH} as given by Eq. (14) are plotted against relative density in Fig. 8(b) using dashed lines. Also plotted in the same figures are the data obtained from the recent chamber tests at the Tokyo University of Science and at Chao Tung University in Taiwan. It can be seen that for q_{c1}, the rate of increase in penetration resistance tends to decrease with increase in D_r. Looking over the new data together with the trends given by Eq. (14), it might be possible to draw new lines as shown by solid lines in Fig. 8(b). This is expressed by

$$C_{CPH} = \left(\frac{K_C}{K_{C,NC}} \right)^{0.60-0.55(D_r/100)} \tag{15}$$

Effect of K_C on Liquefaction Resistance

As described by Eq. (1), Ishihara and Takatsu (1979) have shown that the effect of K_C on liquefaction resistance can be expressed as follows:

$$\frac{R}{R_{NC}} = \frac{1+2K_C}{1+2K_{C,NC}} \tag{16}$$

By applying the above equation on the average curves of the liquefaction resistance – relative density relations for fine and coarse sands (see Fig. 7), which can be considered as the reference curves (K_C = 0.5), the effects of K_C on R can be obtained, as shown in Fig. 9, for example.

RELATION BETWEEN PENETRATION RESISTANCE AND LIQUEFACTION RESISTANCE

As mentioned in previous sections, it was possible to establish the basic relationship between penetration resistance and liquefaction resistance at K_C = 0.5 using relative density. Moreover, the effects of K_C on penetration resistance and on liquefaction resistance have also been discussed above. Therefore, the relationship between penetration resistance and liquefaction resistance for different K_C–values can now be established. The liquefaction resistance curves expressed in terms of K_C–values can be formulated by substituting Eqs. (11) and (16) into Eqs. (4) and (5) for N_1 values, and Eqs. (15) and (16) into Eqs. (6) and (7) for q_{c1} values. The plots thus obtained are shown in Figs. 10 and 11, respectively. As seen from Fig. 10(b) , the reference curve (K_C = 0.5) by Youd *et al.* plots higher than the reference curve based on Japanese practice. This may be due to the fact that the liquefaction strength was determined from different sources: the plot of Youd *et al*. was based mainly on field observations while the Japanese curve was obtained from laboratory triaxial test

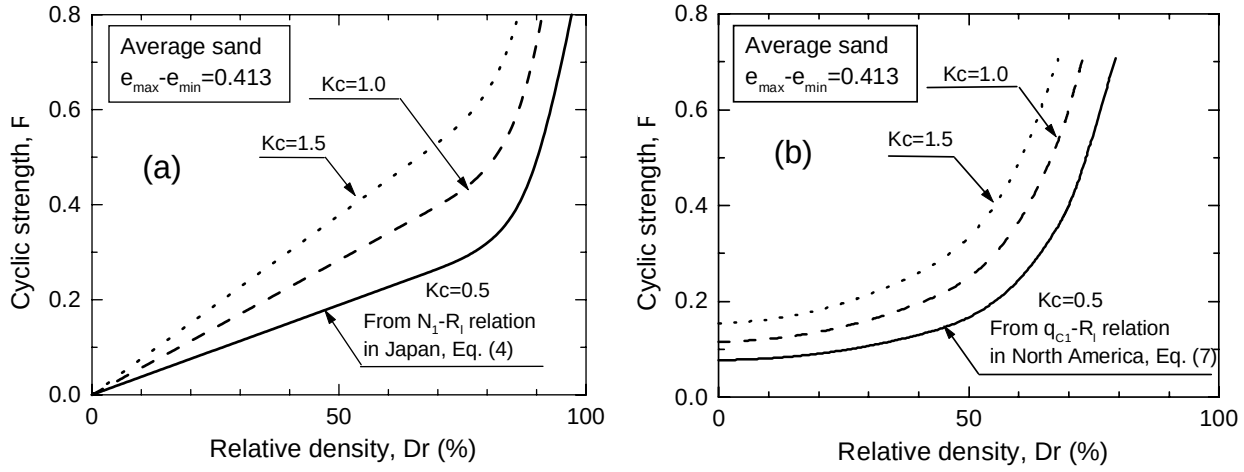

Figure 9: Effect of K_C on liquefaction strength: (a) from Eq. (11); and (b) from Eq. (15).

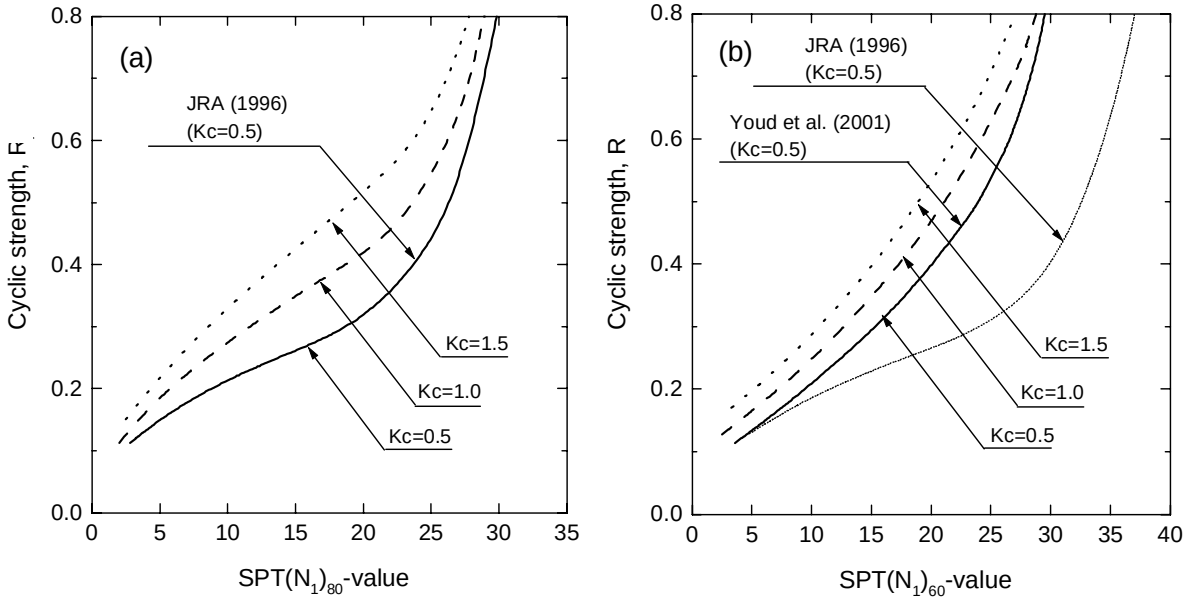

Figure 10: Recommended charts correlating corrected N value and liquefaction strength through K_C.

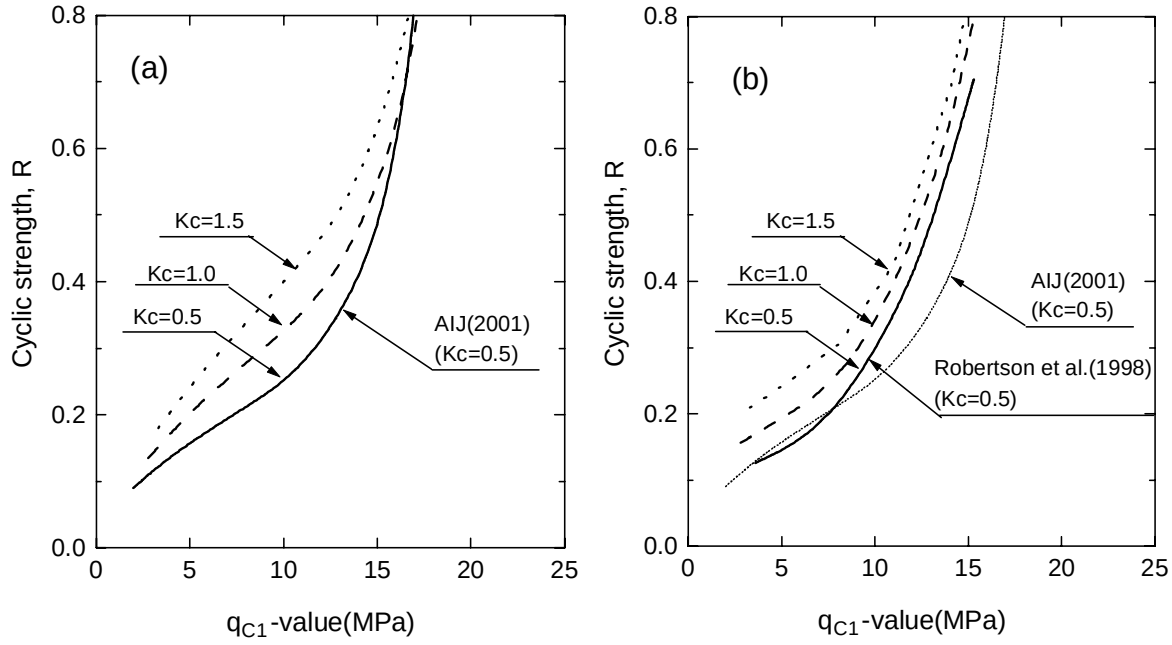

Figure 11: Recommended chart correlating corrected q_c value and liquefaction strength through K_C.

results of high quality undisturbed samples. Another possible reason is that Japanese practice uses 20 cycles as reference for liquefaction resistance, while 15 cycles is tacitly assumed in the US practice. In contrast, the reference curve for K_C = 0.5 based on AIJ specification more or less coincides with that by Robertson–Wride (1998) in the range of q_{c1} smaller than about 10 MPa.

Looking at the effect of lateral stress, it can be seen from the figures that as K_C increases, the liquefaction resistance also increases. It may also be seen that all the curves generally tend to merge to be a curve close to each other at large values of penetration resistance, indicating that the effect of K_C tends to decrease in denser deposits.

To explain this tendency, schematic diagrams showing the effect of K_C on the relationship between liquefaction resistance and penetration resistance are shown in Figs. 12(a) and 12(b) for deposits with low and high penetration resistance, respectively. Suppose the penetration resistance is increased from a value at point a to point b while keeping K_C = 0.5, the liquefaction resistance R is increased from point b to e. If the K_C–value is increased, then additional increase in R is expected, as indicated by the shift from point e to d. It can also be observed that the gradient of the liquefaction curve at point a for K_C = 0.5 is smaller than the gradient due to combined increase in K_C and N_1 or q_{c1} (point a to d). Hence, the liquefaction curve has shifted upwards.

When the ground has low penetration resistance (loose deposits), the gradient due to the increase in K_C is much greater than the gradient coming from the density increase alone. This indicates that the effect of K_C on R is more significant than the effect of penetration resistance for a loose state of deposits as shown in Fig. 12(a). On the other hand, when the ground has high penetration resistance (dense

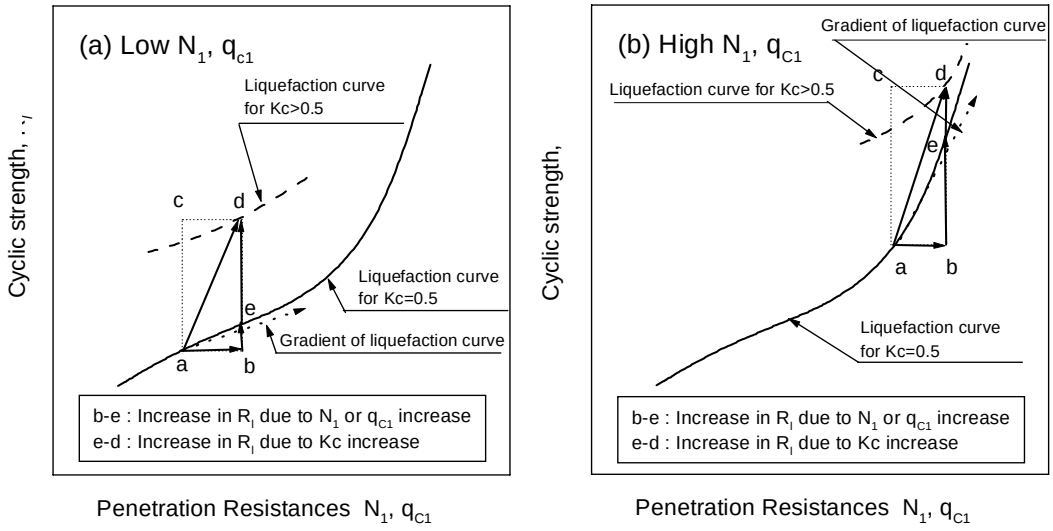

Figure 12: Schematic diagram showing the effect of K_C on penetration resistance and liquefaction resistance.

deposits), the gradient of the liquefaction curve for K_C = 0.5 is generally high, indicating that the effect of penetration resistance is much more significant than the effect of K_C , as illustrated in Fig. 12(b). Thus, it can be said that with increasing K_C–value, the liquefaction resistance increases, but its effect becomes smaller at higher density.

COMPONENTS CONTRIBUTING TO INCREASED LIQUEFACTION RESISTANCE

Based on the above discussion, the increase in liquefaction resistance of ground improved by the sand compaction pile method is due to two components i.e., the increase in penetration resistance and the increase in K_C–values. To expound on this in more detail, the contributions of increased K_C–value and increased penetration resistance on the resulting increase in liquefaction resistance were analyzed quantitatively. Both the liquefaction curves based on Japanese and American practice were considered. For illustration purposes, the data for loose (pre–SCP N_1–value = 5 or q_{c1} = 5 MPa) and medium dense deposits (pre–SCP N_1–value = 15 or q_{c1} = 10 MPa) were evaluated for K_C = 0.5, 1.0 and 1.5.

The results are illustrated in Figs. 13 and 14 for N_1–values based on Japanese and American practice, respectively, while the corresponding results are given in Figs. 15 and 16 for q_{c1}–values, respectively. The left graphs in each figure correspond to low initial (pre–SCP) penetration resistances, while the right graphs are for higher penetration resistances. In the graphs, the vertical axes represent the increase in liquefaction resistance ΔR, while the horizontal axes show the increase in penetration resistance, i.e. ΔN_1 or Δq_{c1}. The numbers indicated in the charts correspond to the contribution of increased penetration or increased K_C–value (from 0.5 to 1.0, or from 1.0 to 1.5). For example, consider the left-most graph on Fig. 13(a), representing a loose deposit (N_1 = 5) prior to SCP implementation. After compaction the N_1–value rose to 10 and such an increase in penetration resistance alone accounted for 54% of the total increase in liquefaction resistance, while the remaining 46% was due to an increase in K_C–value from 0.5 to 1.0. On the other hand, if the K_C–value is increased from 0.5 to 1.5 during SCP implementation, the contribution of the increase in N_1–value to the increase in R is about 39%, while the contributions of the increase in K_C from 0.5 to 1.0 and from 1.0 to 1.5 are 33% and 28%, respectively.

For all figures, it can be observed that the larger the increase in penetration resistance, the increase in liquefaction resistance becomes higher. However, compared to the contribution of increase in the K_C–values, the contribution of increase in penetration resistance is relatively more significant, accounting for about 50–80% of the increase in liquefaction resistance in the case of the high increase in penetration resistance (e.g., if ΔN_1 = 15 or 20, or Δq_{c1} = 7.5 or 10 MPa). Moreover, it is observed that such trend is stronger when the initial penetration resistance is high or if the penetration testing is done through CPT. Similar trends were observed for the charts correlating R and N_1 or q_{c1} based on North American practice.

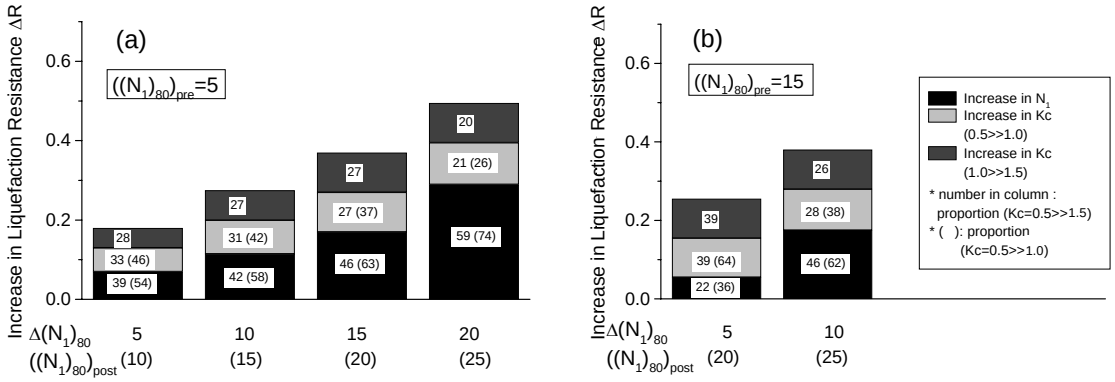

Figure 13: Plots showing the contributions of increased N_1–value and K_C–value on the increase in R for grounds with (a) low and (b) high initial SPT N_1–values (based on Japanese practice).

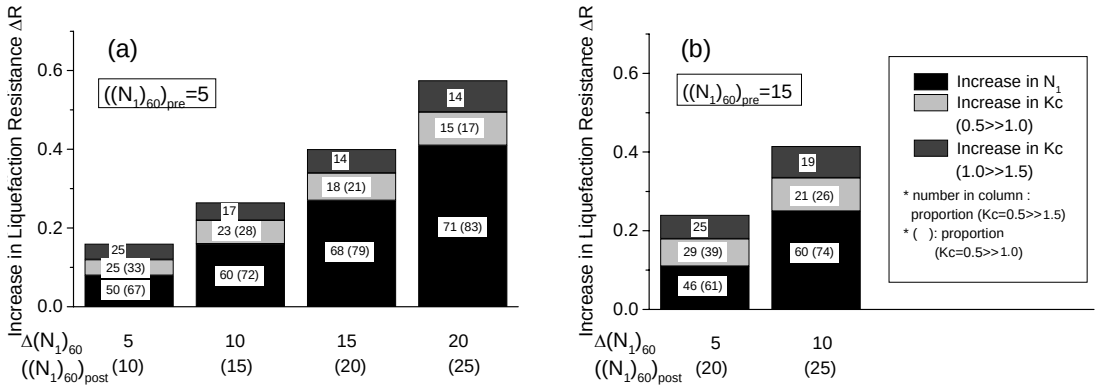

Figure 14: Plots showing the contributions of increased N_1–value and K_C–value on the increase in R for grounds with (a) low and (b) high initial SPT N_1–values (based on American practice).

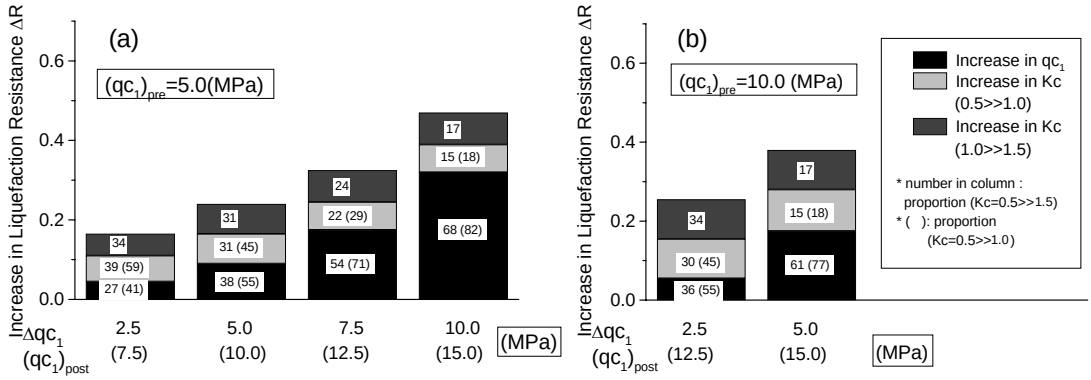

Figure 15: Plots showing the contributions of increased q_{c1}–value and K_C–value on the increase in R for grounds with: (a) low and (b) high initial CPT q_{c1}–values (based on Japanese practice).

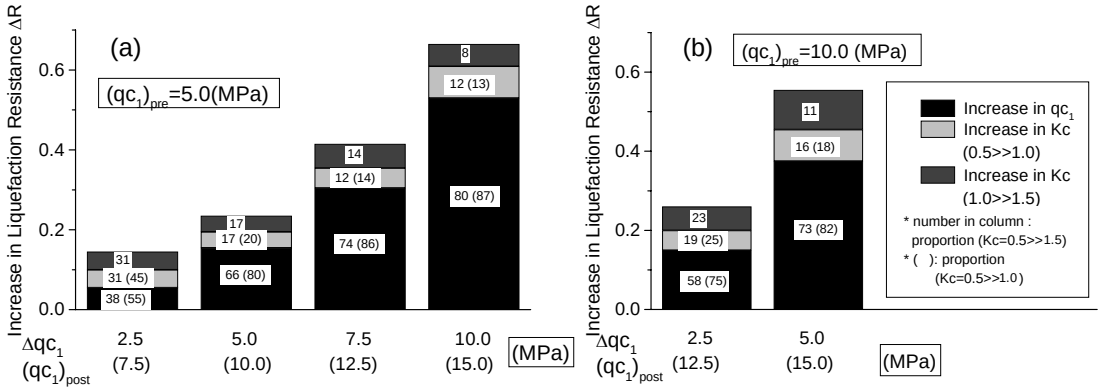

Figure 16: Plots showing the contributions of increased q_{c1}–value and K_C–value on the increase in R for grounds with: (a) low and (b) high initial CPT q_{c1}–values (based on American practice).

In practice, the magnitude of the lateral stress in ground improved by compaction methods can be obtained using dilatometer, pressuremeter and similar equipment. Once the penetration resistance and the K_C–value are known, the corresponding liquefaction resistance of the improved ground can be determined from the design charts to evaluate the potential to liquefaction. Care must be taken in interpreting the results because, as observed in Fig. 3, the K_C–value can change with time, as a result of stress relaxation and other factors.

It is worthy to mention that the proposed charts have been derived based on assumptions which require further validation and on empirical correlations containing significant scatter and uncertainties. Hence, users must be aware of these limitations when employing these charts in important design projects.

CONCLUDING REMARKS

In order to examine the effects of K_C–states on the penetration resistances and liquefaction resistance of ground improved by the sand compaction pile method, experimental data from chamber tests with controlled K_C–values were compiled and arranged. From the curves relating penetration resistances (N_1 and q_{c1}) and relative density, as well as those relating liquefaction resistance and relative density, charts were formulated showing the relationship between liquefaction resistance and penetration resistances as functions of the K_C–values.

Based on a detailed analysis of the charts, it was observed that if the increase in penetration resistance due to SCP is larger, the contribution of increased K_C to the increased liquefaction resistance becomes smaller. These charts can be used to

quantify the effects of increase in lateral stress on the liquefaction resistance of grounds improved by the sand compaction pile method.

Although quite straight forward, the proposed charts are limited by the assumptions used, which need further verification. Furthermore, the charts have been developed for clean sand deposits and the applicability of this study to ground containing some amount of fines would be an issue to be pursued in more detail in future studies.

REFERENCES

1 Architectural Institute of Japan, AIJ, (2001). *Recommendations for Design of Building Foundations*, p.65 (in Japanese).

2 Boulanger, R. W., (2003). "High overburden stress effects in liquefaction analysis," *J. Geot Eng, ASCE*, **129** (12), 1071–1082.

3 Cubrinovski, M. and Ishihara, K. (1999). "Empirical correlation between SPT N–value and relative density for sandy soils," *Soils and Foundations*, **39** (5), 61–71.

4 Fujita, K., (1968). "Standard penetration test," *Interpretation of Soil Investigation Test Results and Example Application, JSSMFE*, 29–76 (in Japanese).

5 Gibbs, H.J. and Holtz, W.G., (1957). "Re-search on determining the density of sand by spoon penetration test," *Proc. 4th International Conference on Soil Mechanics and Foundation Engineering*, Vol. **1**, 35–39.

6 Harada, K., Yasuda, S., Yamamoto, M., Arai, D. and Uda, M., (2000). "Influence of earth pressure coefficient on SPT–N value and liquefaction resistance of the ground improved by compaction methods," *Proc., GeoEng2000*.

7 Huang, A.B. and Hsu, H.H., (2005). "Cone penetration tests under simulated field conditions," *Geotechnique*, **55** (5), 345–354.

8 Ishihara, K. and Takatsu, H., (1979). "Effects of overconsolidation and KO conditions on the liquefaction characteristics of sands," *Soils & Foundations*, **19** (4), 59–68.

9 Ishihara, K., (1996). *Soil Behaviour in Earthquake Geotechnics*, Oxford Press, 209–218.

10 Jamiolkowski, M., Ghionna, V.N., Lancellotta, R. and Paqualisis, E., (1988). "New correlations of penetration tests for design practice," *Proc. Int Symp on Penetration Testing, ISOPT–1*, Orlando, Balkema, 263–296.

11 Japan Road Association, JRA (1996). "Part V, Seismic Design," *Specifications for Highway Bridges* (in Japanese).

12 Meyerhof, G.G., (1957). "Discussion on research on determining the density of sands by penetration testing," *Proc., 4th International Conference on Soil Mechanics and Foundation Engineering*, London, U.K., Vol. III, 110.

13 Robertson, P.K. and Wride, C.E., (1998). "Evaluating cyclic liquefaction potential using the cone penetration test," *Canadian Geotechnical Journal*, **35**(3), 442–459.

14 Salgado, R., Boulanger R.W. and Mitchell, J.K., (1997). "Lateral stress effects on CPT liquefaction resistance correlations," *Journal of Geotechnical Engineering, ASCE*, **123** (8), 726–735.

15 Suzuki, Y. and Tokimatsu, K., (2003). "Correlations between CPT data and liquefaction resistance of in–situ frozen samples," *J. Struct Constr Eng, AIJ*, **566**, 81–88 (in Japanese).

16 Yasuda, S., Nishikawa, O., Kobayashi, T., Asaka, H. and Naito, F., (1996). "Model tests on the relation between relative density and SPT N–value," *Proc., 51st Annual Conference of JSCE*, 290–291 (in Japanese).

17 Yoshida, T. and Kokusho, T., (1988). "Proposal on the method of application of penetration test on sandy ground," *CRIEPI Report* (in Japanese).

18 Youd, T.L., Idriss, I.M., Andrus, R.D., Arango, I., Castro, G., Christian, J.T., Dobry, R., Liam Finn, W.D.L., Harder, L.F. Jr., Hynes, M.E., Ishihara, K., Koester, J.P., Liao, S.S.C., Marcuson, W.F. III, Martin, G.R., Mitchell, J.K., Moriwaki, Y., Power, M.S., Robertson, P.K., Seed, R.B., Stokoe, K.H. II, (2001). "Liquefaction Resistance of Soils: Summary Report from the 1996 NCEER and 1998 NCEER/NSF Workshops on Evaluation of Liquefaction Resistance of Soils," J*ournal of Geotechnical and Geoenvironmental Engineering, ASCE*. **127** (10), p 817–833.